Electronic Supplementary Information (ESI)

Active Bioparticle Manipulation in Microfluidic Systems

Mohd Anuar Md Ali, [a] Kostya (Ken) Ostrikov, [bc] Fararishah Abdul Khalid, [d] Burhanuddin Y. Majlis [a] and Aminuddin A. Kayani *[aef]

[a]*Institute of Microengineering and Nanoelectronics, Universiti Kebangsaan Malaysia, Bangi, Selangor 43600, Malaysia.*
Email: burhan@ukm.edu.my
[b]*School of Chemistry, Physics, and Mechanical Engineering, Queensland University of Technology, Brisbane QLD 4000, Australia.*
Email: kostya.ostrikov@qut.edu.au
[c] *CSIRO-QUT Joint Sustainable Materials and Devices Laboratory, P. O. Box 218, Lindfield NSW 2070, Australia.*
[d] *Faculty of Technology Management and Technopreneurship, Universiti Teknikal Malaysia Melaka, Melaka 75300, Malaysia.*
Email: fararishah@utem.edu.my
[e] *Center for Advanced Materials and Green Technology, Multimedia University, Melaka, Melaka 75450, Malaysia.*
Email: aminuddin.kayani@mmu.edu.my
[f] *School of Electrical and Computer Engineering, RMIT University, VIC 3001, Australia.*

Corresponding Author:
Dr. Aminuddin A. Kayani, Center for Advanced Materials and Green Technology, Multimedia University, Melaka, Melaka 75450, Malaysia. aminuddin.kayani@mmu.edu.my

Electronic Supplementary Information Contents

1. Features and Function of Bioparticles
2. Bioparticle Active Manipulation Forces
3. Bioparticle Manipulation Features and Criteria

1 Features and Function of Bioparticles

Table S1 Features and functions of bioparticles

Bioparticles	Features	Functions
Red blood cells (RBC), White blood cells (WBC)	RBC: Size between 6-8 μm.[1] WBC: Size between 10-20 μm according to WBC type.[1]	RBC: Transportation of oxygen, hormones, nutrients, as well as waste, carbon dioxide and heat. WBC: Protecting body from pathogens and other foreign substances that enter the body.
Cancer cells, Tumor cells	Large nucleus, irregular size and shape, prominent nucleoli, scarce cytoplasm and intense or pale colour.[2]	Malignant when natural killer cells fail to recognize and destroy them.
Stem cells	Cells with the ability to self-renew and differentiate.[3]	Adult stem cells maintain the organ or tissue in which they reside throughout the lifespan. Pluripotent stem cells generate any type of cell found in the body for organ and tissue repair.
Viruses	Genes enclosed by a protective coat. Size between 15 to 200 nm. Contain either double- or single-stranded DNA or RNA.[1,4,5]	Infective agent.
DNA, RNA	Groups of nucleic acids, made from nucleotides.[1] DNA: Double-stranded molecule with a long chain of nucleotides. RNA: Single-stranded molecule with shorter chain of nucleotides.[1]	Carry genetic information. DNA: Storing and transferring genetic information. RNA: Messenger between DNA and ribosomes to make proteins.
Proteins	Biomolecules made from a single or a number of long chains of amino acids residue.[6]	Catalyzing metabolic reactions, DNA replication, responding to stimuli, and transporting molecules from one location to another.

2 Bioparticle Active Manipulation Forces

We review the fundamentals of active manipulation forces for manipulating bioparticles in microfluidic systems, including: (1) hydrodynamic; (2) electrophoretic; (3) dielectrophoretic; (4) magnetophoretic; (5) acoustophoretic; (6) thermophoretic; forces and (7) optical tweezing.

2.1 Hydrodynamic

Hydrodynamic (HYD) forces originate from liquid motion.[7,8] HYD forces can provide precision particle motions under laminar flow in microfluidic system and may separate bioparticles according to their size and mass.[9,10]

Reynolds number, Re_d, which is the ratio of inertial to viscous forces determine the flow regime, whether it is laminar or turbulent. Re_d is governed by eqn (1), where, ρ_m is the medium density, v_f is the average velocity of the medium, L is the microfluidic channel's equivalent diameter, and μ_m is the dynamic viscosity of the medium.[8,11] Laminar flow exhibits at Re_d range less than 1000.

$$Re_d = \frac{\rho_m v_f L}{\mu_m} \tag{1}$$

Bioparticles experience two dominant forces, namely the viscous drag force, F_D, and the inertial lift force, F_L, during movement through a fluid. Viscous drag force, F_D, propels the particle along the flow streamlines. F_D effects upon a spherical particle is estimated by Stokes law, given in eqn (2), where, a is the particle radius, and U_p is the relative velocity between the particle and the surrounding medium.

$$F_D = 6\pi\mu_m a U_p \tag{2}$$

The inertial lift force, F_L, on the other hand, pushes the particles across the streamlines. F_L is the net lift force due to the balance between the wall-induced lift force, and the shear-induced lift force. The net force causes the particles to converge to an equilibrium position between the microfluidic channel centerline and sidewall. F_L is given by eqn (3), where, C_L is lift coefficient that depends on fluid density that surrounds the bioparticle.[7,8]

$$F_L = \frac{4\rho_m C_L v_f^2 a^4}{3\pi\mu_m L^2} \tag{3}$$

In some cases, the flow profile is influenced by secondary flow drag force. One such example is the transverse secondary flow occurring in a curved channel. In this case, the secondary flow manifests as a pair of counter-rotating vortices positioned symmetrically above and below the channel mid-plane.[12] The rotating flow is characterized by the Dean number, κ, which expresses the relative magnitude of inertial and centrifugal forces to viscous forces. κ is governed by eqn (4), where, $\delta = d/R$, R is radius of the flow path radius curvature.

$$\kappa = \delta^{0.5} Re_d \tag{4}$$

At a very low flow rate ($\kappa \sim 1$) centrifugal effects are weak and do not influence the axial laminar profile. As the flow rate increases, transverse flow component acts to transport fluid from the inner wall of the channel radially toward the outer walls. At the channel centerline where axial velocity is maximum, the centrifugal effects are greatest which results in outward flow along the mid-plane while slower-moving fluid near the sidewalls is simultaneously swept inward. At the end of such channels, two parallel fluid streams can entirely switch positions because of an almost complete 180° rotation that is being induced.

The geometrical structure of the microfluidic channel is one of the factors contributing to how the bioparticles are manipulated in HYD manipulation. Other factors include externally driven pressure or flow control. Typical geometries for microchannels include straight,[13] curved,[14] spiral,[15] asymmetric curves[16] and contraction-expansion[17] channels. Each geometry can impose different magnitude and change of wall-induced lift force, shear-induced lift force and secondary flow drag force along the channel, giving capability to conduct desired manipulation.[8]

HYD forces are used in sheathless alignment, cell separation or fractionation, fluid exchange, mixing and volume reduction.[8,14,18,19] One critical example of manipulation of bioparticles using the HYD force is the isolation of circulating tumor cells (CTCs) from blood, demonstrated by Sollier et al.[17] They used dimension change in the form of contraction and expansion of the microchannel to induce the imbalance between wall-induced lift force and the shear-induced lift force. The imbalance forces result in the formation of a vortex to trap CTCs into reservoir due to greater lateral displacement of CTCs as they are larger compared to blood cells.

An example of the manipulation of bioparticles using HYD is depicted in Fig. S1a.

2.2 Electrophoresis

Electrophoresis is the motion of charged particles in a fluid under the influence of an electric field.[20,21] Electrophoretic (EP) force has the advantage of low sample and buffer requirement, high separation efficiency, versatility, sensitivity and short analysis time. It has limitations where it requires the suspending medium to be conductive and usually the availability of the compound of interest is limited by the complexity of the purification procedure and the cost of synthesis. Salt solution, weak acids or weak bases are regularly used as suspending medium for bioparticle manipulation.[20,22,23]

Electrophoresis is generated by a pair of electrodes connected to a direct current (DC) power source onto suspended particles in an ionic solution. When the electrical field is applied, the EP force, F_{EP} is generated. F_{EP} moves the charged particle to the electrode having the opposite charge polarity. The induced motion depends on the polarity and magnitude of the net electrical charge of the particle. However, the net force depends on the combined effect with friction force, F_{FR}, and electrophoretic retardation force, F_{RET}. The friction force F_{FR} is the viscous force, which depends on the suspending medium viscosity and the particle size, whereas, the retardation force F_{RET} is the force that exerted on the diffused cloud of ions with opposite charge polarity to the particle that surrounds it, known as the *Debye layer*. F_{RET} causes a fluid flow with direction that oppose the F_{EP}. This results in a frictional drag that retards the electrophoretically induced motion.[11]

Electrophoretic mobility, μ_{EP}, is the measure of charged particle mobility under electric field. When a particle is suspended in a low Reynolds number medium while a moderate electrical field E applied, the EP mobility, μ_{EP}, experienced by the particle is given in eqn (5), where υ is velocity of the suspended particle.

$$\mu_{EP} = \frac{\upsilon}{E} \tag{5}$$

Smoluchowski[24] developed electrophoretic mobility theory which is valid for the case of sufficiently thin *Debye layer*, where the particle radius, a, is much greater than *Debye length*, κ^{-1} ($a \gg \kappa^{-1}$). The electrophoretic mobility in this theory is governed by eqn (6), where ε_m is the dielectric constant of the suspending medium, ε_0 is the permittivity of free space, η is dynamic viscosity of the suspending medium, and ζ is zeta potential.

$$\mu_{EP} = \frac{\varepsilon_m \varepsilon_0 \zeta}{\eta} \tag{6}$$

For the case of a thick *Debye layer*, where the particle radius is much smaller than the *Debye length* ($a << \kappa^{-1}$), the electrophoretic mobility is governed by Hückel's theory, which is given in eqn (7).

$$\mu_{EP} = \frac{2\varepsilon_m \varepsilon_0 \zeta}{3\eta} \tag{7}$$

The zeta potential, ζ, the electrokinetic potential in colloidal dispersions, is governed by eqn (8), where, σ is the conductivity of the suspending medium.

$$\zeta = \frac{\sigma \alpha}{\varepsilon_m (1 + \alpha\kappa)} \tag{8}$$

The EP force has been applied in various bioparticle manipulations such as in bacteria focusing and immobilization which demonstrated by Oukacine et al.[25] and micro RNAs separation demonstrated by Ban et al.[26] EP force has also been widely used for DNA fingerprinting,[27,28] drug analysis[29,30] and protein characterization.[31–33]An example of manipulation of bioparticles using the EP force is depicted in Fig. S1b.

2.3 Dielectrophoresis

Dielectrophoresis is the motion of polarizable particles induced by a spatially non-uniform electric field.[21,34,35] Particles are temporarily polarized, establishing dipoles which induce unequal Columbic forces causing the particles to move.[11,36,37] The dielectrophoretic (DEP) force can assemble particles into forming suspended objects such as strings, chains or clusters in liquid.

The classical DEP force, F_{DEP}, which is valid for a stationary alternative-current (AC) field is given in eqn (9), where E is the electric field, ε_m is the permittivity of the suspending medium and a is the particle radius, f_{CM} is the Clausius–Mossotti (CM) factor, describing relationship between dielectric constants of two different media.

$$F_{DEP} = 2\pi a^3 \varepsilon_m f_{CM} \nabla |E|^2 \tag{9}$$

For a spherical particle, f_{CM} is governed by eqn (10), where ε is the permittivity, and subscripts ''p'' and ''m'' stand for the particle and the medium, respectively.

$$f_{CM} = \frac{\varepsilon_p - \varepsilon_m}{\varepsilon_p + 2\varepsilon_m} \tag{10}$$

The DEP force is proportional to particle volume, and is highly dependent on the electrical properties of the particle and medium, and the frequency of the field. The polarity of the DEP force depends on the sign of the CM factor, f_{CM}.[38] If f_{CM} is positive ($F_{DEP}>0$), particles will be attracted to the region of high electric field gradients, and this phenomenon is known as positive DEP (pDEP). Conversely if f_{CM} is negative ($F_{DEP}<0$), particles will be repelled from those regions, and this is known as negative DEP (nDEP).

For an AC field that has spatial variation, the DEP force is given by eqn (11), where, Re[f_{CM}] is the real part of f_{CM}, Im[f_{CM}] is the imaginary part, φ is the phase of the AC-field, and subscript i refers to each component of the electric field and the phase gradient. The last term in the parenthesis is a tensor notation and it refers to the summation of the components of the vector quantities inside the bracket.[38]

$$F_{DEP} = 2\pi\varepsilon_m Re[f_{CM}] a^3 \nabla |E|^2 + 2\pi\varepsilon_m Im[f_{CM}] a^3 \times \left(|E_i|^2 \nabla \varphi_i\right) \tag{11}$$

The AC field with spatial variation is being applied in travelling wave DEP (twDEP) and electrorotation (ER) manipulation. The twDEP is typically generated by applying 90° phase-shifted voltages (0°, 90°, 180°, and 270° phase-shifted) on a planar parallel electrode array. In twDEP a travelling wave of electrostatic potential is generated that can suspend a lossy dielectric sphere vertically while simultaneously propelling it along the array. The ER is generated by quadrupole (90° phase shifted voltages) electrodes. When the electrodes are excited with this multiphase AC voltage, a rotating electric field is generated. In twDEP, Im[f_{CM}] determines the translational movement in direction of electrodes array, while Re[f_{CM}] determines whether the bioparticles are levitated (nDEP) or attracted to electrodes (*pDEP*). In ER, typical manipulation is achieved using nDEP (Re[f_{CM}]<0) to levitate the bioparticles during the rotational motion which is determined by Im[f_{CM}].[39]

In the case of the DEP force effect on bioparticle, the particles' permittivity to be used for calculating f_{CM} is the overall permittivity of the bioparticle, taking into account the permittivity of all layers, as bioparticles are typically multilayered due to presence of multilayer membranes. For a spherical multilayered particle (such as mammalian cells) the overall permittivity, ε_p is given by eqn (12), where, ε_{pn} is the particle's permittivity including the outermost layer of the bioparticle, while ε_{pn-1} is particle permittivity including until the second outermost layer, excluding outermost layer. a_n is the outermost layer (membrane) radius, and a_{n-1} is the second outermost layer (membrane) radius. The denotation $n= 0,1,2,3\ldots$ is the correspond layer calculation number, and the calculation starts from the smallest layer, n=0. The comprehensive permittivity ε_p is final layer calculated permittivity, ε_{pn}, which is when n is the final layer number.[39]

$$\varepsilon_p = \varepsilon_{p_n}\left[\left(\frac{a_n}{a_{n-1}}\right)^3 + 2\left(\frac{\varepsilon_{p_{n-1}} - \varepsilon_{p_n}}{\varepsilon_{p_{n-1}} + 2\varepsilon_{p_n}}\right)\right] \Big/ \left[\left(\frac{a_n}{a_{n-1}}\right)^3 - \left(\frac{\varepsilon_{p_{n-1}} - \varepsilon_{p_n}}{\varepsilon_{p_{n-1}} + 2\varepsilon_{p_n}}\right)\right] \tag{12}$$

Transition between the pDEP and nDEP responses of bioparticle occurs when the polarization of the particle and the suspending medium are the same. This occurs at a certain frequency, which is called crossover frequency, f_{xo}. For the case of a spherical structure, f_{xo} is governed by eqn (13), where σ_m is the conductivity of the surrounding medium, a is the particle radius and C_m is the capacitance of the bioparticle plasma membrane, which per unit area is typically in the range of 10^{-2} (Fm^{-2}).[40]

$$f_{xo} = \frac{\sqrt{2}\sigma_m}{2\pi a C_m} \tag{13}$$

The process of applying the DEP force external stimuli is highly selective, label-free, quick and low-cost in fabrication.[11,36,41,42] Disadvantages associated with DEP manipulation are related to controlling bioparticles in the nanoscale regime, and the risk of bioparticle damage due to exposure to strong electric fields.[43,44] A recent study has demonstrated the application of discontinuous dielectrophoresis to minimize the damage to cells.[45] Dielectrophoresis has been successfully used for cancer cell detection, leukaemia cell separation and fractionation of cells and proteins.[46–48] An interesting example of bioparticle manipulation using dielectrophoresis is the capture and sorting of CTCs and lymphocytes using DEP cages developed by Fabbri et al.[49] The DEP cages are generated using microelectrode arrays. An example of manipulation of bioparticles using the DEP force is depicted in Fig. S1c.

2.4 Magnetophoresis

Magnetophoresis is the motion of particles due to exposure to a non-uniform magnetic field. The target

bioparticle is magnetized during this exposure and is either pushed toward the regions of high magnetic flux density or repelled from them. The suspending medium is generally a magnetic or immuno-magnetic liquid such as iron oxide, saline, or phosphate buffered saline (PBS).[11,50–53] Magnetic field can be generated by a permanent magnet or an electromagnetic coil.

The magnetophoretic (MAG) force experienced by a particle is governed by eqn (14), where, F_{MAG} is the magnetic force acting on the particle, χ_p and χ_m are the magnetic susceptibility of the particle and the medium, respectively, V_p is the volume of the particle, B is the magnetic flux density, and μ_0 is the permeability of free space.[54]

$$F_{MAG} = \frac{(\chi_p - \chi_m)V_p}{\mu_0}(B \cdot \nabla)B \tag{14}$$

The particle influenced by MAG force is either pushed towards high magnetic flux density region or repelled from it. The motional direction is determined by the magnetic susceptibility difference between the particle and the medium, χ_p-χ_m. When the magnetic susceptibility difference is positive (χ_p-χ_m>0), the suspended particles are pushed to areas where magnetic field flux gradient is maximum. The phenomenon is called positive magnetophoresis (pMAG). In contrast, when magnetic susceptibility difference is negative, (χ_p-χ_m<0) the suspended particles are pushed to areas where magnetic field flux gradient is minimum, and the phenomenon is known as negative magnetophoresis (nMAG).

Typical practice in bioparticle manipulation using magnetophoresis is either by using paramagnetic microparticles, known as immuno-magnetic bioparticle manipulation, or by using paramagnetic or ferro-fluid suspending media, known as diamagnetic bioparticle manipulation.[55–58] Magnetic materials are divided into three categories, including ferromagnetic, paramagnetic and diamagnetic. Diamagnetic materials are materials that have no magnetic moments. However, when exposed to a magnetic field, a negative magnetization is produced which may induce an internal magnetic field opposite to the direction of the external fields. Paramagnetic materials experience a magnetic moment in the direction of the external magnetic field which results in a positive magnetization and magnetic susceptibility. These materials become magnetized when exposed to an external magnetic field however, do not retain their magnetization when the field is removed. Unlike paramagnetic materials, ferromagnetic materials become magnetized and remain magnetized even after the external magnetic field is removed. These materials experience parallel alignment of magnetic moments to the external magnetic field resulting in strong exchange of forces and very strong magnetic interactions.[59]

In immuno-magnetic bioparticle manipulation, paramagnetic microparticles, such as iron oxide microparticles and streptavidin paramagnetic particles with high susceptibility compared to suspending medium are used. In this method, targeted bioparticles are attached to paramagnetic microparticles through antibodies, which have binding affinity to bioparticles. When exposed to a magnetic field, the microparticles attached to bioparticles can be manipulated. A study by Schneider et al.[60] showing the manipulation of immuno-magnetically labelled leukaemia cells is a good example.

In diamagnetic bioparticle manipulation, a suspending medium with high magnetic susceptibility compared to targeted bioparticle is used. In this method, the magnetic field manipulates the suspending medium rather than the bioparticles themselves. Zeng et al.[61] demonstrated the manipulation of yeast cells using this method.

Magnetophoresis is generally preferred for bioparticle manipulation, as magnetic particles can bind to a targeted bioparticle. Magnetic nanoparticles have been widely used for *in vivo* drug delivery applications

involving cellular therapy, tissue repair, hyperthermia and magnetofection. These nanoparticles have high magnetic susceptibility that allow a targeted delivery with particle localization in specific areas.[62] **The** nature of surface coating and their subsequent geometric arrangement on the nanoparticles determine not only on the size of the colloid but also play a significant role in bio kinetics and distribution of nanoparticles in patients' tissue or cells. Magnetic nanoparticles can bind to drugs, proteins, enzymes, antibodies and nucleotides, and can be directed to an organ, tissue or tumor using an external magnetic field, or can be heated in alternating magnetic fields for hyperthermia. Precise drug delivery to the exact area of inflammation is desirable since this could lead to reduced drug dosage, elimination of side effects and shortens the recovery time.

Additionally, the MAG force is also preferred as it is non-invasive, does not cause bioparticle latency, and can induce angular rotation and positioning.[63–65] However, bioparticles may suffer a hysteresis effect, which causes agglomeration after the magnetic stimuli is removed.[65]

Examples of bioparticle manipulation using the MAG force, are include enrichment of red blood cells (RBCs) from blood using native magnetic properties of RBCs demonstrated by Jung et al.[66] and monitoring growth of *Escherichia coli* (*E. coli*) bacteria which attached to magnetic bead and controlled with rotational motion in electromagnetic coil demonstrated by Kinnunen et al.[67] An example of bioparticle manipulation using the MAG force is depicted in Fig. S1d.

2.5 Acoustophoresis

Acoustophoresis is the movement of bioparticles when exposed to a surface acoustic wave (SAW) radiation pressure, either in travelling surface acoustic wave (TSAW) or standing surface acoustic wave (SSAW) mode.[47] A TSAW occurs when a SAW is propagating from interdigitated transducer (IDT) electrodes. In the case of a SSAW, two TSAW constructively interfere and form a standing or stationary SAW. TSAW is generated by a single IDT electrode, while the SSAW can be generated either by a pair of IDT electrodes or a combination of a single IDT and wave reflectors.[68,69] In TSAW acoustophoresis, bioparticles move together with the propagation of the SAW, while in a SSAW acoustophoresis, bioparticles are pushed toward the SAW pressure node or the pressure antinode. Pressure node is the region of constant pressure, while pressure antinodes are regions alternating between maximum and minimum pressure values.[70]

The magnitude of acoustophoretic (ACT) force experienced by a particle is governed by eqn (15), where F_{ax} is the acoustic radiation force, E_{ac} is the acoustic energy density, a is the particle radius and x is the distance from pressure antinode in the wave propagation axis, k is the wave number ($2\pi f l c_0$) and φ is the acoustic contrast factor.[71]

$$F_{ax} = 4\pi a^3 E_{ac} k \sin(2kx)\varphi \tag{15}$$

The direction of particle movement, whether pushed towards the pressure node or pressure antinode, is determined by the sign of the acoustic contrast factor, φ, which is governed by eqn (16), where ρ_p and ρ_0 are density of the particle and medium, respectively, c_p and c_0 are the speed of sound within the particle and medium, respectively. When the acoustic contrast factor is positive (φ>0), the particles are pushed toward pressure node, and the phenomenon is called positive acoustophoresis (pACT). In contrast, when the acoustic contrast factor is negative (φ<0), the particles are pushed towards the pressure antinode, and the phenomenon is known as negative acoustophoresis (nACT).

$$\varphi = \frac{\rho_p + \frac{2}{3}(\rho_p - \rho_0)}{2\rho_p + \rho_0} - \frac{1\rho_0 c_0^2}{3\rho_p c_p^2} \tag{16}$$

ACT force is non-invasive and versatile, requires simple fabrication procedures, and is convenient to integrate with lab-on-chip (LOC) microfluidic devices.[72] Acoustophoresis faces the challenge of isolating and separating rich combinations of bioparticles such as numerous types of bioparticles residing in a microfluidic suspension.[73]

Acoustophoresis has been applied to numerous biomedical applications, such as plasma protein removal and isolation of low-molecular-weight compounds from red blood cells (RBCs),[74] separation of heterogeneous cell mixtures in continuous flow,[75] separation of lymphocyte subsets from peripheral blood progenitor cells,[76] and trapping and aggregation of lung cancer cells.[77] One fascinating example is the separation of cancer cells from white blood cells (WBCs) demonstrated by Antfolk et al.[78] based on the size, density and compressibility difference of the cells. An example of bioparticle manipulation using ACT force is depicted in Fig. S1e.

2.6 Thermophoresis

Thermophoresis is the motion of particles driven by thermal gradients in the suspending medium. Thermal gradients are usually generated locally by absorption of infrared (IR) laser. The thermal gradients cause the particles move by diffusion, either towards higher or lower temperature medium. Studies show that a temperature difference between 2 to 8 K in the beam center with a $1/e^2$ diameter of 25 μm managed to induce thermophoretic (THM) motion.[79,80] The $1/e^2$ diameter (e=2.71828) is the diameter of beam where intensity falls to 13.5% of the maximum value. The temperature rise of the suspending medium must be kept low to avoid damaging of bioparticles, such as in the case of DNA, it is from 23 to 31°C.[81]

Liquid flow density, J driven by THM field, is given in eqn (17), where, D is diffusion coefficient, c is concentration, T is temperature, and S_T is the Soret coefficient, defined as the ratio of thermal diffusion coefficient, D_T, over diffusion coefficient, D, which is given in eqn (18).

$$J = D[\nabla c + S_T c(1 - c)\nabla T] \tag{17}$$

$$S_T = \frac{D_T}{D} \tag{18}$$

Steady state concentration changes for a given spatial temperature difference, ΔT is given by eqn (19), where, c_{hot} is molecule concentration in the hot area, while c_{cold} is in the cold area.

$$\frac{c_{hot}}{c_{cold}} = exp(-S_T \Delta T) \tag{19}$$

THM manipulation is favoured due to being label-free, immobilization-free and applicable for sub-cell manipulation.[82,83] However, THM has limitations, including difficulty in transporting low concentrations of bioparticles and the system must be free from convective flows.[84] THM platforms have been utilized for quantifying binding affinities, analyzing bio molecular interactions and modifying sub-cell molecules, including proteins or DNA.[80,82,85]

An example of bioparticle manipulation using the THM force is demonstrated by the work of Reichl and Braun[82] where they manipulated molecular movement in living cells using temperature gradients and the representation of molecular diffusion driven by the THM force is depicted in Fig. S1f below.

2.7 Optical tweezing

The process of manipulating bioparticles using optical forces is commonly known as optical tweezing (OPT), which refers to using light radiation pressure to displace and demobilize target bioparticles.[58,86,87]

Light emitted by a light source, causes scattering and gradient forces, which affect particle in the light propagation axis. Scattering force, F_{scat} works in the direction of propagation, where the particle is pushed away from the light source. Gradient force, F_{grad}, on the other hand, works in the direction of the OPT field gradient, resulting in the particle being attracted to region of peak spatial light intensity.

There are two separate explanations for OPT manipulation, which are based on the dimension of particle size with respect to optical wavelength. The first explanation relates to the *Mie* regime condition, where particle dimensions are greater than the wavelength of light, ($d >> \lambda$), can be explained by ray-optics. Manipulation of cell type bioparticles lies on this regime. Rays of light carry momentum and refracted when pass through a particle with a refractive index, n_2, which greater than the surrounding medium, n_1. The rate of change of momentum in the detected rays develop an equal and opposite rate of change in momentum to the particle, due to conservation of momentum, producing a force by Newton's Second Law. When a particle is placed in a light gradient, the sum of all rays passing through it creates an imbalance in force, which push the particle towards the higher intensity region of light. A focus develops a trap because the strong light gradient points towards the center.[88]

The second explanation relates to the *Rayleigh* regime condition, where particles are very small compared to wavelength ($d << \lambda$). In this regime, the particles can be considered as an infinitesimally induced point dipoles that interact with the light field resulting from polarization in homogeneous electrical field.[87] In a homogeneous electric field E, the induced dipole moment, p_{dipole}, by polarization is given in eqn (20), where, n_1 is refractive index of suspending medium, n_2 is refractive index of the particle, a is radius of the particle, ε_0 is permittivity in vacuum and m is the index contrast ratio, where $m = n_2 / n_1$.

$$p_{dipole} = 4\pi n_1^2 \varepsilon_0 a^3 \left(\frac{m^2 - 1}{m^2 + 2}\right) E \tag{20}$$

The magnitudes of scattering force, F_{scat}, and gradient force, F_{grad}, based on point dipole interaction with light field method are given by eqn (21) and eqn (22), respectively, where, I is light intensity, c is speed of light, k is wave number ($k=2\pi/\lambda$) and λ is wavelength.[87]

$$F_{scat} = \frac{8\pi n_1 k^4 a^6}{3c} \left(\frac{m^2 - 1}{m^2 + 2}\right) I \tag{21}$$

$$F_{grad} = \frac{2\pi n_1 a^3}{c} \left(\frac{m^2 - 1}{m^2 + 2}\right) \nabla I \tag{22}$$

Trapping is achieved at the highest intensity axis when $F_{grad} > F_{scat}$. OPT works by light emission through a high numerical aperture number (NA) microscope objective (MO), which focuses light tightly and results in a force along the highest intensity axis, but in the backward direction, which causes the bioparticle to be demobilized.[87]

The OPT force is applied to control bioparticles without mechanical contact and can be classified as a label-free method.[58,89] OPT manipulation has the advantage of high precision motion and immobilization. However, it has the disadvantage of being confined to handle low volume of samples and poses the risk of damaging

bioparticles due to over-exposure of optical electromagnetic fields and over-heating of the cells.[90,91] OPT has been used in alignment of cell's nucleus, trapping of bacterial cells, 3D micro patterning of biological structures and single-molecule studies of DNA.[92,93] However, in DNA studies, the molecules are typically bound to microspheres because even though the contour length of DNA is commonly at least several mm, the molecule's axial diameter is only around 2 nm. The microspheres are optically trapped and moved to induce stretch on DNA.[94] The example is stretching of DNA using double-tweezer as demonstrated by Gupta et al.[95] Each DNA end is attached with a polystyrene (PS) bead and each PS beads is trapped in an optical tweezer to induce the stretch. Fig. S1g shows a pictorial example of bioparticle manipulation using OPT forces.

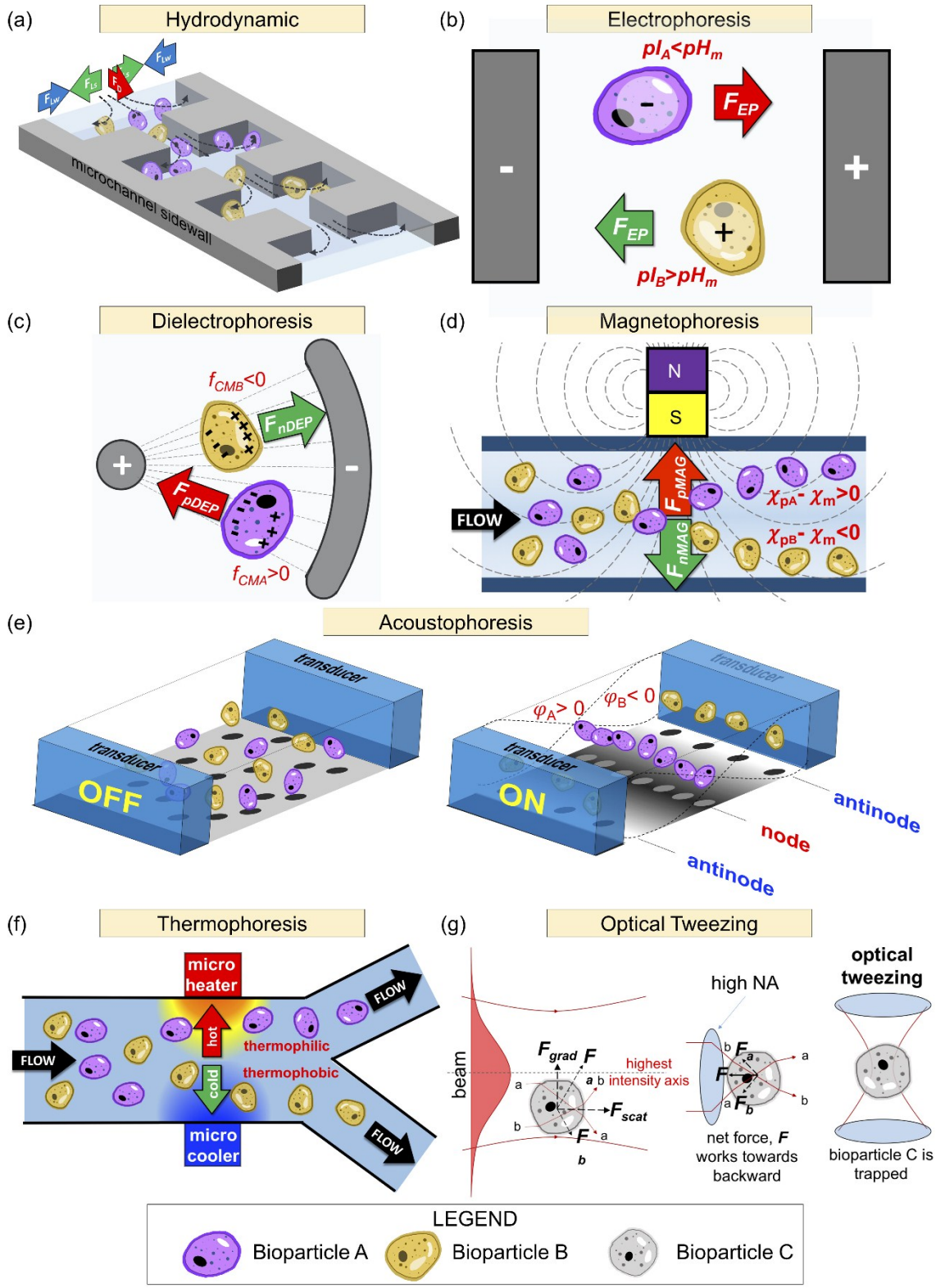

Fig. S1 Bioparticle active manipulation forces. (a) Hydrodynamic. (b) Electrophoresis. (c) Dielectrophoresis. (d) Magnetophoresis. (e) Acoustophoresis. (f) Thermophoresis. (g) Optical tweezing. Detailed caption available in the main manuscript.

3 Bioparticle Manipulation Features and Criteria

Table S2 Bioparticle manipulation features and criteria

Bioparticle	Features	Manipulation criteria
Model organisms	HYD manipulation which highly depends on particles size has the advantage of manipulating model organisms which are relatively large compared to other organisms. ACT forces can induce translocation and immobilization of model organisms using ACT focusing or microwell.	HYD manipulation based on model organism size. ACT manipulation is based on organism density or compressibility.
Blood cells	DEP forces can manipulate mixture of blood cells. In fact, DEP forces also can manipulate same type of cell with different deformability caused by infection. MAG forces can manipulate RBCs selectively.	DEP manipulation based on electric properties between different type of blood cells. MAG manipulation of RBCs as RBCs exhibit magnetic properties.
Tumor and cancer cells	DEP forces can manipulate based on electrical properties difference between cancerous cell and non-cancerous cells. Tumor and cancer cells show change in compressibility or deformability, differ from non-cancerous cells, thus exhibit contrast response to ACT forces. However, biofunctionalized particle can be used to enhance selectivity of cancer cells trapping using ACT forces.	Cancer cells and non-cancerous cells exhibit different electrical characteristics. ACT manipulation is based on the difference of density between cancer cells and non-cancerous cells.
Stem / progenitor cells	MAG forces can manipulate stem cells with desired configuration such as levitated differentiation, by using biofunctionalized magnetic micro- or nano-particles to bind with the stem cells.	MAG force takes advantage of the affinity reaction between stem cells and biomarker.
Bacteria	MAG forces are advantageous for bacteria manipulation because it can target specific bacteria based on affinity reaction with bounded biomarker.	MAG force takes advantage of the affinity reaction between bacteria and biomarker.
Viruses	MAG forces can manipulate virus when biofunctionalized micro- or nano-particle react with the virus based on antigen-antibody reaction.	MAG force takes advantage of the affinity reaction between virus and biomarker.
Nucleic acids	OPT forces can induce stretch of DNA for DNA studies. THM forces have the capability of manipulating sub cell bioparticles.	OPT and THM forces manipulate biofunctionalized particle to bind with nucleic acids.
Proteins	Protein manipulation at the current stage still depends on binding with biomarkers, thus needs a biofunctionalized magnetic micro/nano particle to carry be manipulated using the MAG forces. THM forces can manipulate sub cell bioparticles.	MAG and THM forces manipulate biofunctionalized particle to bind with target proteins.

References

1 B. Alberts, A. Johnson, J. Lewis, M. Raff, K. Roberts, P. Walter, J. Wilson and T. Hunt, *Molecular biology of the cell*, Garland Science, New York, 5th edn., 2008.

2 A. I. Baba and C. Câtoi, in *Comparative Oncology*, The Publishing House of the Romanian Academy, Bucharest, 2007.

3 D. J. Barfoot, E. Kemp, K. Doherty, P. C. Blackburn, D. S. Sengoku, A. Van Servellen, D. A. Gavai and D. A. Karlsson, *Stem Cell Research - Trends and Perspectives on the Evolving International Landscape*, 2013.

4 G. P. Rédei and G. Rédel, *Encyclopedia of genetics, genomics, proteomics, and informatics*, Springer, New York, 2008.

5 A. W. Artenstein, *Vaccines: A Biography*, Springer Science+Business Media, New York, 2010, vol. 34.

6 D. Whitford, *Proteins : structure and function*, J. Wiley & Sons, Hoboken, NJ, 2005.

7 J. Zhou and I. Papautsky, *Lab Chip*, 2013, **13**, 1121–1132.

8 J. M. Martel and M. Toner, *Annu. Rev. Biomed. Eng.*, 2014, **16**, 371–396.

9 S. Kakaç, B. Kosoy, D. Li and A. Pramuanjaroenkij, *Microfluidics Based Microsystems: Fundamentals and Applications*, Springer Netherlands, Dordrecht, 2009.

10 J. Alvankarian, A. Bahadorimehr and B. Yeop Majlis, *Biomicrofluidics*, 2013, **7**, 14102.

11 A. A. Kayani, K. Khoshmanesh, S. A. Ward, A. Mitchell and K. Kalantar-zadeh, *Biomicrofluidics*, 2012, **6**, 31501.

12 A. P. Sudarsan and V. M. Ugaz, *Proc. Natl. Acad. Sci.*, 2006, **103**, 7228–7233.

13 S. Bose, R. Singh, M. Hanewich-Hollatz, C. Shen, C.-H. Lee, D. M. Dorfman, J. M. Karp and R. Karnik, *Sci. Rep.*, 2013, **3**, 2329.

14 M. E. Warkiani, A. K. P. Tay, G. Guan and J. Han, *Sci. Rep.*, 2015, **5**, 11018.

15 S. S. Kuntaegowdanahalli, A. A. S. Bhagat, G. Kumar and I. Papautsky, *Lab Chip*, 2009, **9**, 2973–2980.

16 J. M. Martel, K. C. Smith, M. Dlamini, K. Pletcher, J. Yang, M. Karabacak, D. A. Haber, R. Kapur and M. Toner, *Sci. Rep.*, 2015, **5**, 11300.

17 E. Sollier, D. E. Go, J. Che, D. R. Gossett, S. O'Byrne, W. M. Weaver, N. Kummer, M. Rettig, J. Goldman, N. Nickols, S. McCloskey, R. P. Kulkarni and D. Di Carlo, *Lab Chip*, 2014, **14**, 63–77.

18 M. G. Lee, J. H. Shin, C. Y. Bae, S. Choi and J. K. Park, *Anal. Chem.*, 2013, **85**, 6213–6218.

19 T. J. Causon, L. Maringer, W. Buchberger and C. W. Klampfl, *J. Chromatogr. A*, 2014, **1343**, 182–187.

20 K. D. Dorfman, in *Encyclopedia of Microfluidics and Nanofluidics*, ed. D. Li, Springer US, Boston, MA, 2008, pp. 580–588.

21 J. Voldman, *Annu. Rev. Biomed. Eng.*, 2006, **8**, 425–454.

22 I. O. Neaga, E. Bodoki, S. Hambye, B. Blankert and R. Oprean, *Talanta*, 2016, **148**, 247–256.

23 D.-M. Liu, Y.-P. Shi and J. Chen, *Chinese J. Anal. Chem.*, 2015, **43**, 775–782.

24 Dongqing Li, *Encyclopedia of microfluidics and nanofluidics*, Springer, New York, 2008, vol. 1.

25 F. Oukacine, L. Garrelly, B. Romestand, D. M. Goodall, T. Zou and H. Cottet, *Anal. Chem.*, 2011, **83**, 1571–1578.

26 E. Ban, D.-K. Chae and E. J. Song, *J. Chromatogr. A*, 2013, **1315**, 195–9.

27 C. Chiappetta, M. Anile, M. Leopizzi, F. Venuta and C. Della Rocca, *Clin. Chim. Acta*, 2013, **425**, 93–96.

28 B. Lou, E. Chen, X. Zhao, F. Qu and J. Yan, *J. Chromatogr. A*, 2016, **1437**, 203–209.

29 J. Piešťanský, K. Maráková, M. Kovaľ and P. Mikuš, *J. Chromatogr. A*, 2014, **1358**, 285–292.

30 A. Doomkaew, P. Prapatpong, S. Buranphalin, Y. Vander Heyden and L. Suntornsuk, *J. Chromatogr. Sci.*, 2014, **53**, 993–999.

31 L. Zhang, K. Lawson, B. Yeung and J. Wypych, *Anal. Chem.*, 2014, **87**, 470–476.

32 J. M. Ramón-Sierra, J. C. Ruiz-Ruiz and E. de la L. Ortiz-Vázquez, *Food Chem.*, 2015, **183**, 43–48.

33 A. Shabani, *Res. J. Biotechnol.*, 2015, **10**, 29–35.

34 H. A. Pohl, *Dielectrophoresis : The behavior of neutral matter in nonuniform electric fields*, Cambridge University Press, Cambridge, New York, 1978.

35 T. Z. Jubery, S. K. Srivastava and P. Dutta, *Electrophoresis*, 2014, **35**, 691–713.

36 K. Khoshmanesh, S. Nahavandi, S. Baratchi, A. Mitchell and K. Kalantar-zadeh, *Biosens. Bioelectron.*, 2011, **26**, 1800–1814.

37 R. Vaidyanathan, S. Dey, L. G. Carrascosa, M. J. A. Shiddiky and M. Trau, *Biomicrofluidics*, 2015, **9**, 61501.

38 B. Çetin and D. Li, *Electrophoresis*, 2011, **32**, 2410–2427.

39 T. B. Jones, *IEE Eng. Med. Biol. Mag.*, 2003, 33–42.

40 M. Muratore, S. Mitchell and M. Waterfall, *Biochem. Biophys. Res. Commun.*, 2013, **438**, 666–672.

41 R. Martinez-Duarte, *Electrophoresis*, 2012, **33**, 3110–3132.

42 M. Li, W. H. Li, J. Zhang, G. Alici and W. Wen, *J. Phys. D. Appl. Phys.*, 2014, **47**, 63001.

43 A. Menachery and R. Pethig, *IEEE Proc. nanobiotechnology*, 2005, **152**, 207–211.

44 D. S. Gray, J. L. Tan, J. Voldman and C. S. Chen, *Biosens. Bioelectron.*, 2004, **19**, 771–780.

45 R. Soffe, S. Baratchi, S.-Y. Tang, M. Nasabi, P. McIntyre, A. Mitchell and K. Khoshmanesh, *Sci. Rep.*, 2015, **5**, 11973.
46 M. Javanmard, S. Emaminejad, C. Gupta, J. Provine, R. W. Davis and R. T. Howe, *Sensors Actuators, B Chem.*, 2014, **193**, 918–924.
47 S. Van Den Driesche, V. Rao, D. Puchberger-Enengl, W. Witarski and M. J. Vellekoop, *Sensors Actuators, B Chem.*, 2012, **170**, 207–214.
48 H. J. Mulhall, F. H. Labeed, B. Kazmi, D. E. Costea, M. P. Hughes and M. P. Lewis, *Anal. Bioanal. Chem.*, 2011, **401**, 2455–2463.
49 F. Fabbri, S. Carloni, W. Zoli, P. Ulivi, G. Gallerani, P. Fici, E. Chiadini, A. Passardi, G. L. Frassineti, A. Ragazzini and D. Amadori, *Cancer Lett.*, 2013, **335**, 225–231.
50 H. Yan and H. Wu, in *Encyclopedia of Microfluidics and Nanofluidics*, ed. D. Li, Springer US, New York, 2015, pp. 1696–1701.
51 N. Pamme, J. C. T. Eijkel and A. Manz, *J. Magn. Magn. Mater.*, 2006, **307**, 237–244.
52 F. Carpino, L. R. Moore, M. Zborowski, J. J. Chalmers and P. S. Williams, *J. Magn. Magn. Mater.*, 2005, **293**, 546–552.
53 R. Yang, H. Hou, Y. Wang and L. Fu, *Sensors Actuators B. Chem.*, 2016, **224**, 1–15.
54 S. A. Peyman, E. Y. Kwan, O. Margarson, A. Iles and N. Pamme, *J. Chromatogr. A*, 2009, **1216**, 9055–9062.
55 A. S. Ivanov and A. F. Pshenichnikov, *J. Magn. Magn. Mater.*, 2010, **322**, 2575–2580.
56 S. Tokura, M. Hara, N. Kawaguchi and N. Amemiya, *IEEE Trans. Appl. Supercond.*, 2014, **24**, 1–5.
57 J. Lim, R. D. Tilton, A. Eggeman and S. a. Majetich, *J. Magn. Magn. Mater.*, 2007, **311**, 78–83.
58 B. Çetin, M. B. Özer and M. E. Solmaz, *Biochem. Eng. J.*, 2014, **92**, 63–82.
59 M. Getzlaff, *Fundamentals of magnetism*, Springer, Berlin; New York, 2008.
60 T. Schneider, L. R. Moore, Y. Jing, S. Haam, P. S. Williams, A. J. Fleischman, S. Roy, J. J. Chalmers and M. Zborowski, *J. Biochem. Biophys. Methods*, 2006, **68**, 1–21.
61 J. Zeng, Y. Deng, P. Vedantam, T.-R. Tzeng and X. Xuan, *J. Magn. Magn. Mater.*, 2013, **346**, 118–123.
62 A. K. Gupta and M. Gupta, *Biomaterials*, 2005, **26**, 3995–4021.
63 F. Yu, L. Zhang, Y. Huang, K. Sun, A. E. David and V. C. Yang, *Biomaterials*, 2010, **31**, 5842–5848.
64 B. H. McNaughton, P. Kinnunen, R. G. Smith, S. N. Pei, R. Torres-Isea, R. Kopelman and R. Clarke, *J. Magn. Magn. Mater.*, 2009, **321**, 1648–1652.
65 A. Lenshof and T. Laurell, *Chem. Soc. Rev.*, 2010, **39**, 1203–1217.
66 J. Jung, S. K. Seo, Y. D. Joo and K. H. Han, *Sensors Actuators, B Chem.*, 2011, **157**, 314–320.
67 P. Kinnunen, I. Sinn, B. H. McNaughton, D. W. Newton, M. A. Burns and R. Kopelman, *Biosens. Bioelectron.*, 2011, **26**, 2751–2755.
68 H. Zhu, X. Lin, Y. Su, H. Dong and J. Wu, *Biosens. Bioelectron.*, 2015, **63**, 371–378.
69 G. Destgeer and H. J. Sung, *Lab Chip*, 2015, **15**, 2722–38.
70 L. Gao, C. Wyatt Shields, L. M. Johnson, S. W. Graves, B. B. Yellen and G. P. López, *Biomicrofluidics*, 2015, **9**, 14105.
71 A. Lenshof, C. Magnusson and T. Laurell, *Lab Chip*, 2012, **12**, 1210.
72 S.-C. S. Lin, X. Mao and T. J. Huang, *Lab Chip*, 2012, **12**, 2766–2770.
73 S. Deshmukh, Z. Brzozka, T. Laurell and P. Augustsson, *Lab Chip*, 2014, **14**, 3394–400.
74 M. Tenje, M. N. Lundgren, A.-M. M. A.-M. Swärd-Nilsson, J. Kjeldsen-Kragh, L. Lyxe and A. Lenshof, *Biomed. Microdevices*, 2015, **17**, 1–6.
75 Y. Ai and B. L. Marrone, in *Proc. SPIE*, 2014, vol. 8976, pp. 1–7.
76 A. Lenshof, A. Jamal, J. Dykes, A. Urbansky, I. Åstrand-Grundström, T. Laurell and S. Scheding, *Cytom. Part A*, 2014, **85**, 933–941.
77 M. Ohlin, I. Iranmanesh, A. E. Christakou and M. Wiklund, *Lab Chip*, 2015, **15**, 3341–3349.
78 M. Antfolk, C. Antfolk, H. Lilja, T. Laurell and P. Augustsson, *Lab Chip*, 2015, **15**, 2102–2109.
79 P. Reineck, C. J. Wienken and D. Braun, *Electrophoresis*, 2010, **31**, 279–286.
80 P. Baaske, C. J. Wienken, P. Reineck, S. Duhr and D. Braun, *Angew. Chemie Int. Ed.*, 2010, **49**, 2238–2241.
81 L.-H. Yu and Y.-F. Chen, *Anal. Chem.*, 2015, **87**, 2845–2851.
82 M. R. Reichl and D. Braun, *J. Am. Chem. Soc.*, 2014, **136**, 15955–15960.
83 M. Jerabek-Willemsen, T. André, R. Wanner, H. M. Roth, S. Duhr, P. Baaske, D. Breitsprecher, T. Andre, R. Wanner, H. M. Roth, S. Duhr, P. Baaske and D. Breitsprecher, *J. Mol. Struct.*, 2014, **1077**, 101–113.
84 M. A. Rahman and M. Z. Saghir, *Int. J. Heat Mass Transf.*, 2014, **73**, 693–705.
85 K. Zillner, M. Jerabek-Willemsen, S. Duhr, D. Braun, G. Längst and P. Baaske, in *Functional Genomics: Methods and Protocols*, eds. M. Kaufmann and C. Klinger, Springer New York, New York, 2012, vol. 815, pp. 241–252.
86 A. Ashkin, *Phys. Rev. Lett.*, 1970, **24**, 156–159.
87 M. Woerdemann, in *Structured light fields : applications in optical trapping, manipulation, and organisation*, Springer

Berlin Heidelberg, Berlin; New York, 2012, pp. 5–26.
88 K. Svoboda and S. M. Block, *Annu. Rev. Biophys. Biomol. Struct.*, 1994, **23**, 247–285.
89 S. Baratchi, K. Khoshmanesh, C. Sacristán, D. Depoil, D. Wlodkowic, P. McIntyre and A. Mitchell, *Biotechnol. Adv.*, 2014, **32**, 333–346.
90 K. K. C. Neuman and A. Nagy, *Nat. Methods*, 2008, **5**, 491–505.
91 M. Dienerowitz, L. V. Cowan, G. M. Gibson, R. Hay, M. J. Padgett and V. R. Phoenix, *Curr. Microbiol.*, 2014, **69**, 669–674.
92 E. O. Eriksson, D. Engström, J. Scrimgeour and M. Goksör, *Opt. Express*, 2009, **17**, 5585–5594.
93 X. Liu, J. Huang, Y. Zhang and B. Li, *Sci. Rep.*, 2015, **5**, 11578.
94 J. P. Rickgauer and D. E. Smith, in *Soft Matter Characterization*, eds. R. Borsali and R. Pecora, Springer-Verlag, Berlin, Heidelberg, 2008, pp. 1139–1186.
95 A. N. Gupta, A. Vincent, K. Neupane, H. Yu, F. Wang and M. T. Woodside, *Nat. Phys.*, 2011, **7**, 631–634.